Production of Energetic Electrons in the Process of Photodetachment of F^-

Igor Yu. Kiyan and Hanspeter Helm
Fakultät für Physik, Albert-Ludwigs-Universität, D-79104 Freiburg, Germany
(Received 26 November 2002; published 6 May 2003)

An imaging technique is used to record an energy and angle resolved spectrum of electrons produced by photodetachment of F^- in a strong infrared laser pulse. The spectrum involves contributions from more than 23 excess photon detachment channels. Its higher energy part extends beyond the classical cutoff value, and it appears as a pronounced plateau localized within a small angle along the laser polarization axis. A Keldysh-like theory is able to qualitatively reproduce the spectrum without taking into account the rescattering mechanism. The role of the parity of the initial bound state is discussed.

DOI: 10.1103/PhysRevLett.90.183001 PACS numbers: 32.80.Gc, 32.80.Rm

The process of ionization of an atomic system in a strong laser field represents a hot topic in atomic physics. A striking feature of this process is the production of energetic electrons which compose a plateau in the energy spectrum of photoelectrons (for references, see [1,2]). Detailed experimental investigations of the ionization process were performed in neutral atoms in both the multiphoton and tunnel regimes. For example, under the tunnel regime conditions realized by Walker *et al.* in helium, a plateau was recorded with a cutoff energy on the order of 500 eV [3]. Electrons produced with such an energy require absorption of more than 300 quanta. In the present work we investigate the process of photodetachment of a negative ion. The polarization character of binding forces and the enhanced role of electron correlations in negative ions make this investigation interesting and complimentary to studies on photoionization of atoms.

Despite the complexity of a nonperturbative treatment of the problem of photoionization, the production of energetic electrons has received a simple semiclassical description as being due to the elastic rescattering of the photoelectron on the parent core [4]. According to the semiclassical representation, the electron first appears in the continuum via tunneling as a wave packet with zero group velocity but is subjected to the quiver motion in the field. Disregarding the influence of the core potential, this motion can be described classically. In the oscillating linearly polarized field $F\sin\omega t$, the electron velocity has the form $v = (F/\omega)(\cos\omega t - \cos\omega t_0)$. Here F and ω are the electric strength amplitude and the frequency of the field, respectively, and t_0 is the instant of birth of the wave packet. The second, constant term in the above expression represents a drift velocity. The corresponding drift energy represents the electron kinetic energy observed in a short pulse experiment. Without further interaction of the ejected electron with the core, the drift energy can reach a maximum value of $F^2/2\omega^2$, which is twice the ponderomotive energy, U_p. A substantial increase in the drift energy is accomplished in the elastic rescattering process, when the electron wave packet is turned back to the core under the action of the field. Analysis of classical electron trajectories shows that the drift energy acquires its maximum value when the electron is backscattered from the core, and this value is on the order of $10U_p$. The rescattering model was instructively discussed by Kopold *et al.*, who applied a quantum path analysis to the description of high-order channels of ionization from a short-range potential [5]. Their analytical method employed the Keldysh approximation extended to allow for the rescattering effect. Results of the improved Keldysh theory are in agreement with the exact solution of the problem considered, obtained in terms of the quasistationary quasienergy state approach [6].

An important issue in the application of the rescattering model is a proper description of the spatial distribution of the wave packet which is, to a significant extent, defined by the wave function of the initial state. This issue, together with a proper calculation of the scattering amplitude in the Coulomb potential, was considered before [3]. In negative ions, however, the rescattering mechanism is governed by parameters of different value. On one hand, the initial size of the wave packet is larger. This results in a smaller spread of the electron density distribution at the moment when the electron returns back to the core. On another hand, the scattering amplitude is smaller because of the short-range character of the core potential and the absence of the Coulomb focusing [7].

Because negative ions have low binding energies and can be easily destroyed by a laser field of moderate intensity, the experimental investigation of high-order processes in such fragile systems poses specific requirements. A short description of earlier experiments on photodetachment in a strong laser field can be found in Ref. [8]. High saturation intensity conditions can be obtained by reducing the interaction time of ions with the laser field and by using a low laser frequency in order to increase the lowest order of nonlinearity of the process. Thus, an experiment on photodetachment in a strong field requires application of a short laser pulse of infrared frequency. In the present work we expose F^- to a short laser pulse of 1.8 μm wavelength. This negative ion has a binding energy of 3.401 188 7 eV [9], and it requires absorption of at least five infrared photons to overcome the detachment threshold. The high nonlinearity of the

lowest order channel increases the saturation intensity and, thus, reduces the depletion of negative ions at the leading front of the laser pulse. In this way, we are able to record an angle resolved spectrum of photoelectrons which extends up to kinetic energies of approximately 16 eV, corresponding to absorption of 23 excess photons. The higher energy part of the spectrum exhibits a highly pronounced plateau localized along the laser polarization axis. The aim of this work is to discuss the origin of this plateau.

Negative ions of fluorine are extracted from a hollow cathode glow discharge operated with a gas mixture of CF_4 and krypton. The ion beam is accelerated to a kinetic energy of 3 keV, mass analyzed in a Wien filter, and admitted into an ultrahigh vacuum chamber. Differential pumping allows us to maintain the interaction chamber at 2×10^{-10} mbar during the experiment. The typical ion current measured in the interaction region is on the order of 150 nA. At the position of the laser focus the ion beam is focused to a waist of approximately 0.4 mm size. An electron imaging spectrometer (EIS) is used to detect electrons produced in the process of photodetachment. In order to improve the image resolution, the EIS is operated in the velocity mapping regime. It is achieved by creating a nonuniform electrostatic field in such a way that it projects all electrons produced with the same momentum vector into the same point on the position sensitive detector, regardless of the initial electron position in the interaction region. Thus, image broadening due to the finite size of the interaction volume is prevented. Also, the EIS is operated under a hard projection condition with the projection quality parameter ρ exceeding 100 even for the most energetic electrons detected. Here $\rho = eU/E$ is the ratio of the electron energy gained by acceleration in the electrostatic field to the energy gained in the photoprocess. This hard projection practically eliminates image distortion due to the kinematic effect of the moving target. A great reduction in the collisional electron background is achieved by gating on the detector gain in a time window of 20 ns.

Linearly polarized laser pulses of 138 fs (FWHM) duration and 1.8 μm wavelength are generated in an optical parametric amplifier pumped with a mode-locked Ti:sapphire laser at a 1 kHz repetition rate. The pulse energy in the interaction region is 60 μJ. The laser beam is focused with a 15 cm focal length lens and its polarization axis is parallel to the detector plane. The focus size is measured by scanning a razor blade across the focus. It is well approximated by a Gaussian shape with a width of 58 μm (FWHM) and a Rayleigh range of 2.5 mm. The peak intensity in the interaction region is 1.1×10^{13} W/cm^2.

The image processing involves a conventional Abel inversion routine [10]. Using the recorded 2D distribution of electrons in the (x, y) plane of the detector, this procedure reproduces their distribution in the (r, θ) coordinates before projection. Here r is the radius of the expanded electron cloud which is defined by the product of the electron velocity gained in the photoprocess and the time of flight to the detector, and θ is the emission angle with respect to the laser polarization. It is essential that the distribution is axially symmetric and its symmetry axis is perpendicular to the projection field. For a given geometry and voltage setup of the EIS, the radius r is a measure of the electron momentum. The radial scale was calibrated by recording electrons produced in a one-photon detachment of H^- in a weak field at three known wavelengths [8]. The measured calibration coefficient is used to convert the radial scale into the momentum scale.

The upper part of Fig. 1 shows the angular and momentum distribution of photoelectrons obtained as a result of the Abel inversion of the raw image recorded in the present experiment. The excess photon detachment peaks are not resolved in the spectrum because of their large ponderomotive broadening. At the peak intensity the ponderomotive energy is 3.20 eV, while the photon energy is 0.689 eV. The spectrum extends up to electron momenta of 1.08 a.u., corresponding to a kinetic energy of approximately 16 eV. Such an energy is reached via absorption of 23 excess photons. Taking into account the ponderomotive shift of the continuum threshold, the highest order detachment channel recorded in this experiment involves absorption of approximately 32 photons. Contributions of yet higher order processes succumb in the background signal. The momentum spectrum separates into two distinct parts. The lower energy part has a cutoff at the momentum value of 0.7 a.u.. The corresponding energy of 6.6 eV is approximately twice the ponderomotive energy. This part is followed by a plateau localized along the laser polarization axis. Though the signal level in the plateau region is lower by an order of magnitude, its existence demonstrates for the first time the production of energetic electrons in photodetachment. The plateau part of the spectrum suggests a contribution from electron rescattering on the parent core as discussed in the introductory section. However, we show below that all features of the measured spectrum can be reproduced by a Keldysh-like theory without taking into account the rescattering effect.

We simulated the photoelectron spectrum by using the analytical expression by Gribakin and Kuchiev for the differential photodetachment rate [Eq. (33) of Ref. [11]]. Their formula can be applied in the case of nonzero values of the angular momentum quantum numbers (ℓ, m) of the electron in the initial bound state. The calculation involves summation over channels with different values of $m = 0, \pm 1$ simulated separately, and the statistical averaging of channels associated with the two different spin-orbit sublevels of the final atomic state, $^2P^o_{1/2}$ and $^2P^o_{3/2}$, respectively. Because of the fine-structure splitting of 50.1 meV, the detachment threshold associated with the upper F($^2P_{1/2}$) state requires absorption of at least six

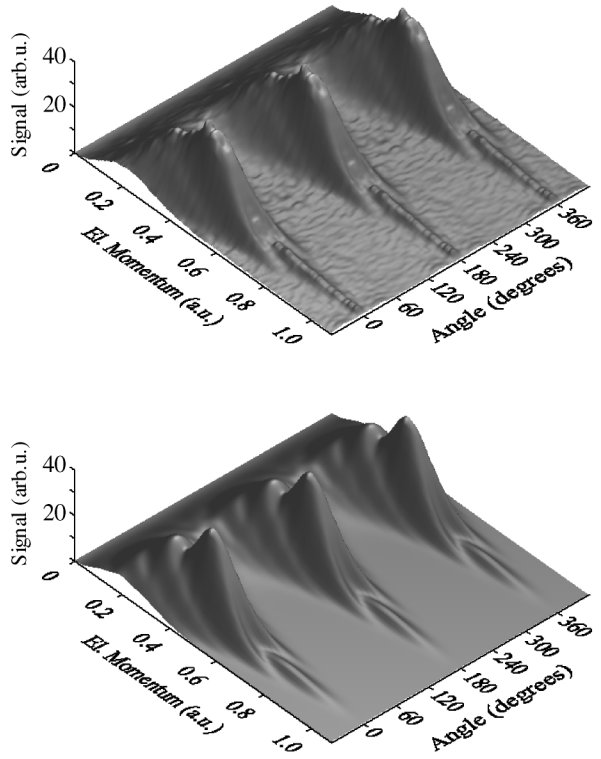

FIG. 1. Angle resolved photoelectron spectrum. The upper part shows the experimental result; the lower part is a simulation using the Keldysh-like theory [11] and explicitly accounting for our experimental parameters.

photons of the central wavelength (1.80 μm), while five photons are sufficient to overcome the F($^2P_{3/2}$) threshold. Nevertheless, the simulation provides similar results in both cases. It can be explained by the fact that the five-photon detachment with the formation of the fluorine atom in the $^2P_{3/2}$ state occurs near the threshold of this process and, thus, is ponderomotively closed at a rather moderate intensity of 1.4×10^{11} W/cm^2. In addition, its contribution is low according to the Wigner threshold law [12]. The theoretical photodetachment rate is integrated over the spatial and temporal intensity distribution in the laser focus. Eventually, the electron distribution is convoluted with the measured response function of the detector to a single electron event. The simulated spectrum is presented in the lower part of Fig. 1. We point out here that the integration over the focal volume is carried out for a focus size of 53 μm (FWHM), which is slightly less than the measured value. The smaller focus size provided a better agreement with the experimental spectrum. Though it might be a matter of precision of the Keldysh-like theory, we cannot exclude a systematic error in the focus measurement related to the pointing instability of the laser beam. The measured focus size is overestimated by 5 μm when the instability is on the order of only 10^{-5} radians. Despite this minor remark, Fig. 1 shows a good qualitative agreement between the theory and our experiment. In particular, the simulation reproduces the plateau part of the spectrum which extends beyond the $2U_p$ energy. It also reproduces well the sidelobes of the lower energy part in the region of its cutoff. We emphasize again that the theory used in this simulation does not take into account the rescattering effect.

In order to explore the rescattering effect under the conditions of our experiment, a similar simulation was performed by using the predictions by Kopold and Becker [13], where an additional interaction of the photoelectron with the residual core is taken into account. However, this theory was developed only for the case of zero value of the initial angular momentum ℓ. As a result of that, the simulated spectrum has a quite different overall shape and is, therefore, not presented here. Instead, we compare results of different simulations with the experimental data in Fig. 2 which shows the kinetic energy distributions along the laser polarization axis. The theoretical curves are normalized to the integrated experimental distribution. The rescattering model (dashed curve) predicts a distinct plateau which dominates in the spectrum at kinetic energies above 12 eV. However, its value is almost 2 orders of magnitude lower than the experimental signal in this region, and well below the experimental background level in Fig. 2 (10^3 arbitrary units (a.u.)). Thus, the rescattering effect can be ruled out as origin of the distinct plateau observed in our experiment. It is interesting to note that at low kinetic energies predictions of the rescattering model coincide with the results of the Gribakin and Kuchiev theory obtained for the case of $\ell = 0$ (dotted curve in Fig. 2). This is due to the fact that

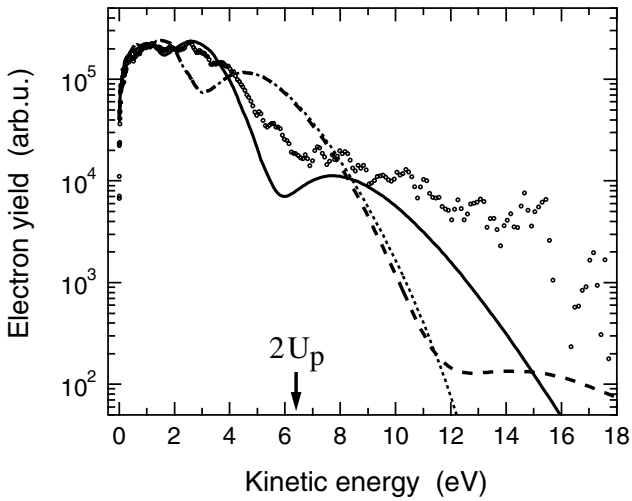

FIG. 2. Energy distribution of photoelectrons emitted along the laser polarization axis. Dots, experimental data; solid line, calculations for $\ell = 1$ [11]; dashed and dotted lines, calculations for $\ell = 0$ with [13] and without [11] the rescattering effect taken into account, respectively. The arrow indicates the classical cutoff energy.

both theories use the same short-range potential model to describe the atomic system.

The discussion above disregards electrons produced by double detachment of F^-. In order to show that this neglect is well justified, we compare total rates of the photodetachment and photoionization processes calculated at the peak intensity. The ionization rate of F is calculated by using the Ammosov-Delone-Krainov (ADK) theory [14] and independently by integrating Eq. (33) of Ref. [11] with the parameter $\nu = (2E_{at})^{-1/2}$ over the solid angle and ionization channels. Here $E_{at} = 0.6404$ a.u. represents the atomic ionization potential. The Keldysh-like theory predicts the ionization rate of an order of magnitude higher than the ADK value. This rate is, however, more than 15 orders of magnitude lower than the photodetachment rate value of 1.5×10^{-4} a.u. Though this consideration implies the sequential scheme of the double detachment, it is quite improbable that the direct double detachment can compensate for such a large number of orders of magnitude.

A comparison of the different predictions presented in Fig. 2 reveals the importance of the parity of the initial state in the process of photodetachment. Except for the plateau contribution, the electron distributions make a few oscillations as a function of the energy. The oscillations are out of phase for $\ell = 0$ and $\ell = 1$, respectively. The simulation performed for the case of $\ell = 1$ (as appropriate for F^-) agrees much better with the experimental data. In particular, it qualitatively reproduces the minimum in the region of the classical cutoff energy (6.4 eV), while simulations performed for the case of $\ell = 0$ predict a maximum at this energy. In order to explore the role of the initial angular momentum ℓ, we expand the analytical formula for the n-photon detachment rate [Eq. (33) of Ref. [11]] in the limit of high kinetic energies, $p^2/2 \gg E_0, U_p$, where $E_0 = \kappa^2/2$ is the binding energy of the initial state. For zero emission angle the first significant term of the expansion acquires the simple form

$$\left.\frac{dw_n}{d\Omega}\right|_{\Theta=0} = \left(\frac{e^3 U_p}{p^2}\right)^n \left[1 + (-1)^\ell \sin\left(\frac{2}{3}\frac{\kappa^3}{\omega p} + \frac{\kappa}{p}\right)\right], \quad (1)$$

where ω is the laser frequency and $p = [2(n\omega - U_p - E_0)]^{1/2}$. Though in our case this expansion is rigorous for energies far above 3 eV, it provides a qualitative explanation of the features observed in the spectrum in the given energy range. Equation (1) shows that the detachment rate, as a function of the electron momentum p, has a factor which oscillates between 0 and 2. The character of its oscillations is determined by the parity of ℓ, as is also apparent from Fig. 2. It also follows from Eq. (1) that at certain values of the electron momentum, when the oscillating factor equals zero, the emission along the laser polarization axis acquires zero probability. In such a case the electron is detached into directions other than the polarization axis. This results in the pronounced sidelobes observed in the experimental and theoretical spectra. The origin of the plateau, as well as of the shoulders embracing each other at lower energies (see the lower part of Fig. 1 for a better resolution), can be described as a result of modulation of a smooth distribution by the oscillating factor. It is interesting to note that for a given parity of the initial state, the momentum, for which emission along the laser polarization axis is zero, is independent of the laser intensity but is solely determined by the laser frequency and the binding energy of the negative ion.

In conclusion, we have shown experimentally that electrons with energies beyond the classical cutoff value are produced in photodetachment of a negative ion. A Keldysh-like theory is able to qualitatively describe the low energy portion and the higher energy plateau part of the spectrum *without* taking into account the rescattering effect. The energy distribution of photoelectrons along the laser polarization axis exhibits an oscillatory behavior consistent with this theory. Its oscillatory character is governed by the parity of the angular momentum quantum number of the electron in the initial ground state. Despite the importance of electron correlations in negative ions, the single-active-electron model reproduces all features of the experimental spectrum. Though the rescattering mechanism was excluded from the interpretation of experimental data, it is desirable to have an improved prediction for this effect when a nonzero initial angular momentum, as well as a realistic potential of the neutral target, is taken into account.

I. Y. K. appreciates communication with G. Gribakin and M. Kuchiev concerning theoretical aspects of this work. This research has been supported by the Deutsche Forschungsgemeinschaft (SFB 276, TPC 14).

[1] N. B. Delone and V. P. Krainov, *Multiphoton Processes in Atoms* (Springer-Verlag, Berlin, 1994).
[2] L. F. DiMauro and P. Agostini, Adv. At. Mol. Opt. Phys. **35**, 79 (1995).
[3] B. Walker *et al.*, Phys. Rev. Lett. **77**, 5031 (1996).
[4] G. G. Paulus *et al.*, J. Phys. B **27**, L703 (1994).
[5] R. Kopold *et al.*, J. Phys. B **35**, 217 (2002).
[6] B. Borca *et al.*, Phys. Rev. Lett. **88**, 193001 (2002).
[7] T. Brabec *et al.*, Phys. Rev. A **54**, R2551 (1996).
[8] R. Reichle *et al.*, Phys. Rev. Lett. **87**, 243001 (2001).
[9] T. Andersen, H. K. Haugen, and H. Hotop, J. Phys. Chem. Ref. Data **28**, 1511 (1999).
[10] C. Bordas *et al.*, Rev. Sci. Instrum. **67**, 2257 (1996).
[11] G. B. Gribakin and M. Yu. Kuchiev, Phys. Rev. A **55**, 3760 (1997).
[12] E. P. Wigner, Phys. Rev. **73**, 1002 (1948).
[13] R. Kopold and W. Becker, J. Phys. B **32**, L419 (1999).
[14] M. V. Ammosov, N. B. Delone, and V. P. Krainov, Sov. Phys. JETP **64**, 1191 (1986).